SAND2022-17075C

First-principle SiPM Characterization to Enable Radiation Detection in Harsh Environments

Jacob Fritchie, Ming Fang, Jon Balajthy, Melinda Sweany, Thomas Weber, and Angela Di Fulvio

***Abstract*—This paper reports the experimental comparison of two silicon photomultipliers (SiPMs): the MicroFJ-30035 by ONSemi and the ASD-NUV3S-P by AdvanSiD, in terms of gain, dark count rate, and crosstalk probability. SiPMs are solid state photon detectors that enable high sensitivity light readout. They have low-voltage power requirements, small form factor, and are durable. For these reasons, they are being considered as replacements for vacuum photomultiplier tubes in some applications. However, their performance relies on several parameters, which need to be carefully characterized to enable their high-fidelity simulation and SiPM-based design of devices capable to operate in harsh environments. The parameters tend to vary between manufacturers and processing technologies. In this work, we have compared the MicroFJ and ASD SiPMs in terms of gain, dark count rate, and crosstalk probability. We found that the dark count rate of the MicroFJ was 16% higher than the ASD. Also, the gain of the MicroFJ is 3.5 times higher than the ASD. Finally, the crosstalk probability of the ASD 1.96 times higher than the MicroFJ. Our findings are in good agreement with manufacturer reported values.**

I. Introduction

Silicon Photomultipliers (SiPMs) are solid-state photodetectors with high single-photon sensitivity and photon detection efficiency over 60% in arrays with large microcells [1], and they are candidates to replace photomultiplier vacuum tubes (PMTs) in applications where low power and form factor are design constraints. Their use in ionizing radiation detection would benefit from high-fidelity, comprehensive models and the characterization of the impact of SiPM electrical properties on the detection properties, such as the energy resolution and pulse shape discrimination.

The sensor of SiPMs is comprised of small microcells, which are themselves avalanche photon detectors operated in Geiger mode. It is necessary to understand how the microcells respond individually to intepret the response of the whole SiPM. By measuring the dark counts of the SiPM, the avalanche response of individual microcells can be measured. Using the resulting signals, a spectrum of the dark count signals is created. The spectrum is then fit with a modified Erlang distribution that is used to extract performance parameters such as the crosstalk probability, avalanche noise, electronic noise, and gain [2]. We have measured the dark count rate (DCR) and extracted the performance parameters of two commercial SiPMs (MicroFJ-30035 by ONSemi and the ASD-NUV3S-P by AdvanSiD) for comparison. These data will be used to model the response of the detection systems encompassing the SiPM.

TABLE I: Parameters for modified Erlang distribution function.

Parameters	Description
p_x	crosstalk probability [%]
σ_e	electronic noise [V]
σ_a	avalanche noise [V]
x_g	gain [V]
x_0	average baseline offset [V]

II. Experimental Methods

A. Dark Count Rate Measurements

Upon interaction with the SiPM microcell, photons create an electron-hole pair in the silicon, which leads to an avalanche of electrons. The electrons are then measured as an electronic signal whose amplitude is correlated to the incident photon energy deposited.

However, electron avalanches can be caused by thermal carriers in the silicon. The thermal carriers create an electron-hole pair that leads to an avalanche and then electronic signal. These events are called dark counts, as they are not caused by a photon. The dark counts create noise, which reduces photon detection efficiency for low light measurements [3]. Furthermore, photons can be generated during the avalanche of electrons. These photons can travel outside of the microcell and travel through the surface protection window of the SiPM to another microcell of an adjacent SiPM. There, they can cause another avalanche, which is referred to as external optical crosstalk. Also, thermal carriers are sometimes created during an avalanche. They can travel through the silicon to a neighboring microcell of the same SiPM and cause an avalanche. This is called internal crosstalk. Both forms are measured as dark counts during a dark count measurement. Studying the dark counts is important to characterize the noisy behavior of the SiPM.

Additionally, measuring the dark counts of a SiPM provides important parameters about the SiPM's performance. By measuring the dark counts, we see signals of one, two, or three photo electron (p.e.) peaks (Fig.1). 1 p.e. corresponds to one

This work is funded in-part by Sandia National Laboratories (LDRD) Award Number 2308289. Sandia National Laboratories is a multimission laboratory managed and operated by National Technology & Engineering Solutions of Sandia, LLC, a wholly owned subsidiary of Honeywell International Inc., for the U.S. Department of Energy's National Nuclear Security Administration under contract DE-NA0003525. This paper describes objective technical results and analysis. Any subjective views or opinions that might be expressed in the paper do not necessarily represent the views of the U.S. Department of Energy or the United States Government.

J. Fritchie, M. Fang, and A. Di Fulvio are with the Department of Nuclear, Plasma, and Radiological Engineering, University of Illinois at Urbana-Champaign, Urbana, IL 61801, United States (e-mail: jwf2@illinois.edu;mingf2@illinois.edu;difulvio@illinois.edu). J. Balajthy, M. Sweany, and T. Weber are with Sandia National Laboratories, Albuquerque, NM 87185, United States (email: jabalaj@sandia.gov;msweany@sandia.gov;tmweber@sandia.gov)

978-1-6654-8872-3/22/$31.00 ©2022 IEEE

microcell firing, 2 p.e. to two microcells, and so on. The amplitude of each peak is then recorded. The peak amplitudes are gathered to form the dark count spectrum.

The MicroFJ pulses has a bandpass filter applied with critical frequencies of $10MHz$ and $3MHz$ (Fig. 2). This allows the peak sample to be picked more accurately. The peak sample of the filtered pulse corresponds to the peak sample in the raw pulse. The amplitude of the raw pulse is used to create the dark count spectrum.

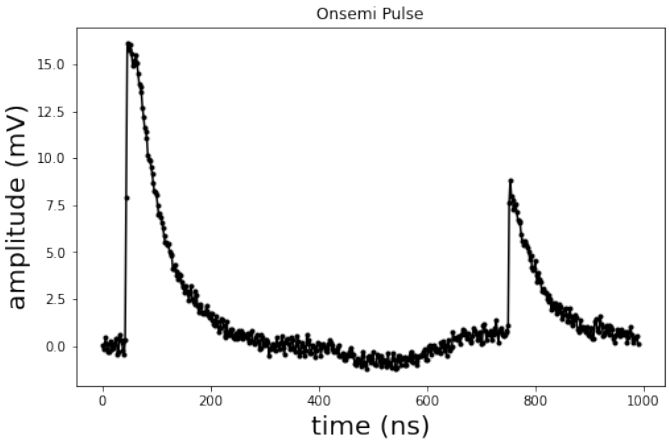

Fig. 1: An example of an Onsemi pulse with a 2 p.e. peak and 1 p.e. peak

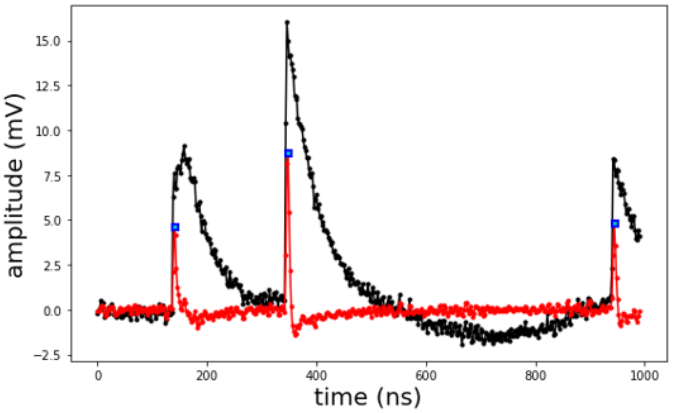

Fig. 2: Raw MicroFJ pulse in black. Bandpass filtered pulse in the red trace.The peak sample is denoted by the blue box.

The ASD pulse is much noisier than the MicroFJ (Fig. 3). The ASD pulses require a lowpass filter for denoising. However, because of the increased noise, the peak sample in the filtered pulse does not correspond to the peak sample in the raw pulse. Therefore, the amplitude of the peak sample in the denoised signal, at the time stamp identified in the filtered signal, is used for the dark count spectrum.

This spectrum can be fit with a modified Erlang distribution [2]. The function is defined by Equation 1

$$Y = A\sum_{n=1}^{\infty}\frac{p_n}{\sqrt{2\pi(\sigma_e^2+n\sigma_a^2)}}\exp\frac{-(x-nx_g-x_o)^2}{2(\sigma_e^2+n\sigma_a^2)} \quad (1)$$

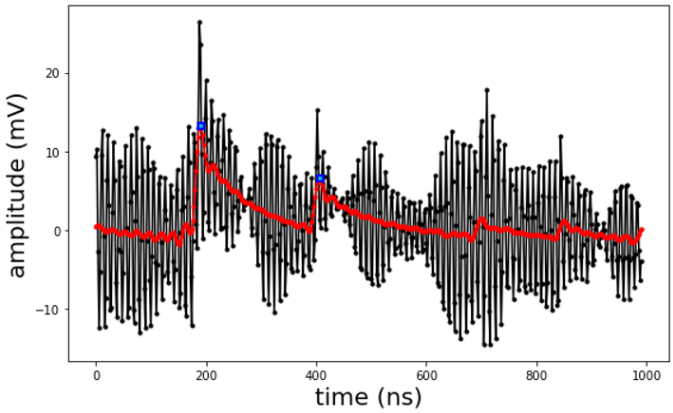

Fig. 3: Raw ASD pulse in black. Lowpass filtered pulse in the red trace.The peak sample is denoted by the blue box.

where the parameters are defined in Table I. The function is a sum of Gaussians that is spread by the electronic noise σ_e and the avalanche noise σ_a.

From the fit, parameters of the SiPM response are extracted, such as the SiPM gain, electronic noise, avalanche noise, and crosstalk probability. These response parameters can be used to compare the performance of different SiPMs.

We measured the DCR of a MicroFJ-30035 (Fig. 6) by ONSemi and an ASD-NUV3S-P (Fig. 7) by AdvanSiD, using the same acquisition setup. The two ASD-NUV3S-P features 5520 microcells and the MicroFJ-30035 features 5676 microcells over a 3mm $\times$ 3mm area, for comparable microcell densities. The setup for this experiment is seen in Fig. 4 for the MicroFJ-30035, and it took place in a dark box (Thorlabs XE25C11). The MicroFJ-30035 was mounted on an MICROFJ-SMA-30035-GEVB evaluation board while the ASD-NUV3S-P was mounted using a passive evaluation board, the schematic of which is seen in Figure 5. The SiPM was biased wwith +5V overvoltage. The signal was output to a low-noise ZFL-1000LN+ amplifier. The amplifier output the signal to a DT5730 CAEN desktop digitizer (14 bits, 500 MSPs), which was connected to a workstation through an optical link to a PCI board.

To trigger on the dark counts, a low threshold must be set on the digitizer. However, this low threshold results in a trigger frequency higher than 1 MHz, which caused buffer overflow and the loss of data by the digitizer. Therefore, a random triggering strategy was used. A CAEN DT5810B Digital Emulator was programmed to output a 10 kHz transistor-transistor logic (TTL) pulse. The TTL pulse was used to trigger the digitizer to acquire data for a window of 992ns. The dark counts were measured for 60s.

When calculating the dark count rate, the duty cycle of the triggering strategy must be taken into account. The dark count rate was calculated as follows:

$$DCR = \frac{P}{d_c t A} \quad (2)$$

where P is the number of peaks at 1 p.e. or above, d_c is the duty cycle, t is the time of acquisition, and A_s is the area of the SiPM sensor.

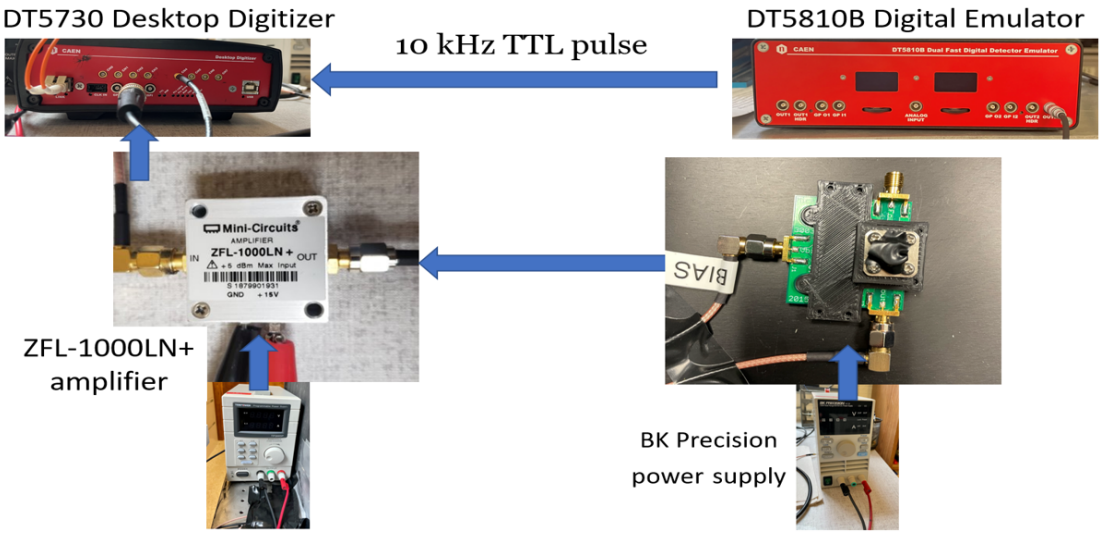

Fig. 4: Diagram of DCR measurement setup.

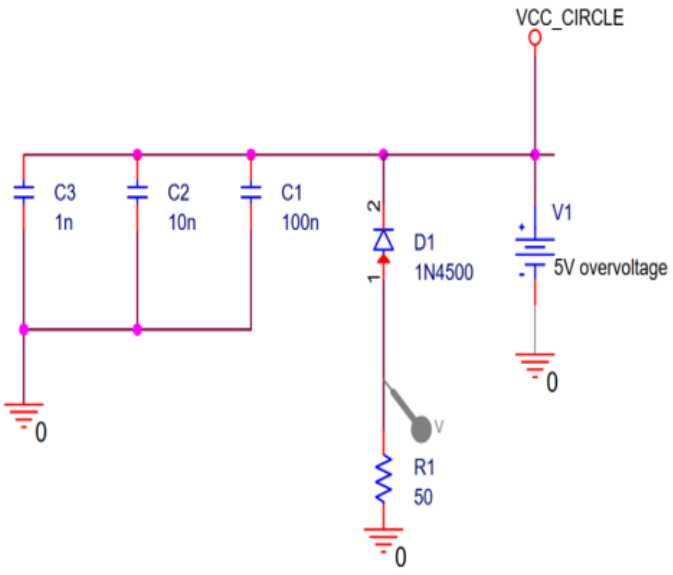

Fig. 5: Schematic of passive evaluation board used for the ASD DCR measurement.

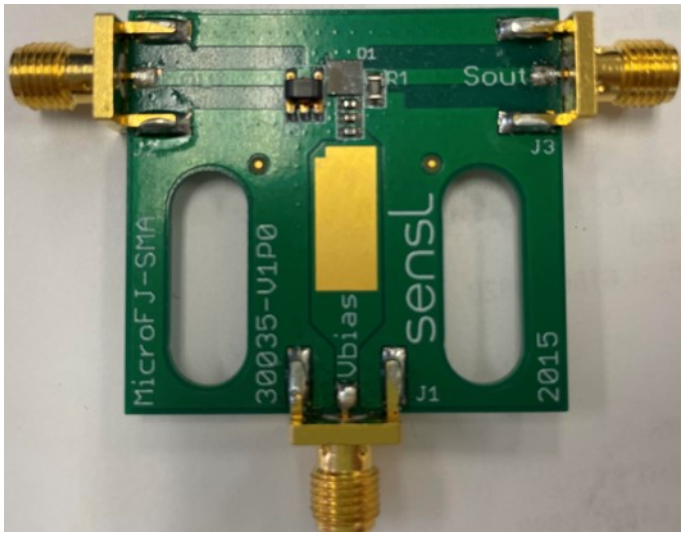

Fig. 6: MicroFJ SiPM mounted on evaluation board.

III. Results

We used the measured data to estimate some of the most important SiPM parameters. These quantities were estimated according to their standard definitions [4]. The DCR results from free charge carriers thermally generated that cause spurious avalanches independent from the illumination field. DCR includes also optical photons developed during an avalanche capable of triggering secondary avalanches. We used the amplitudes of the measured peaks to create the dark count rate spectrum seen in Fig. 8 and Fig. 9.

The MicroFJ spectrum reveals 9 resolvable p.e. peaks. The modified Erlang distribution (Equation 1) fits well to the spectrum. In the ASD spectrum, we can resolve 11 p.e. peaks. However, the ASD peaks are less well-defined than the MicroFJ. This effect could be caused by the increased noise that is seen in the ASD pulses (Figure 3). The resolution of the ASD peaks could be decreased by the use of the denoised peak sample amplitude in the dark count spectrum. The parameters that are extracted from the spectrums are in Table II.

TABLE II: Other extracted parameters from the dark count rate spectrum.

Parameters	MicroFJ value	ASD value
p_x	10.0	19.6
σ_e	1.50mV	0.70mV
σ_a	0.614mV	0.105mV
x_g	7.49mV	2.15mV
x_0	0.719mV	0.515mV

The measured crosstalk probability of the ASD is 19.6%, which is almost twice as high as the MicroFJ of 10.0%. The electronic noise in the MicroFJ is 46.7% higher than the ASD. The avalanche noise 585 % higher in the MicroFJ. The lower

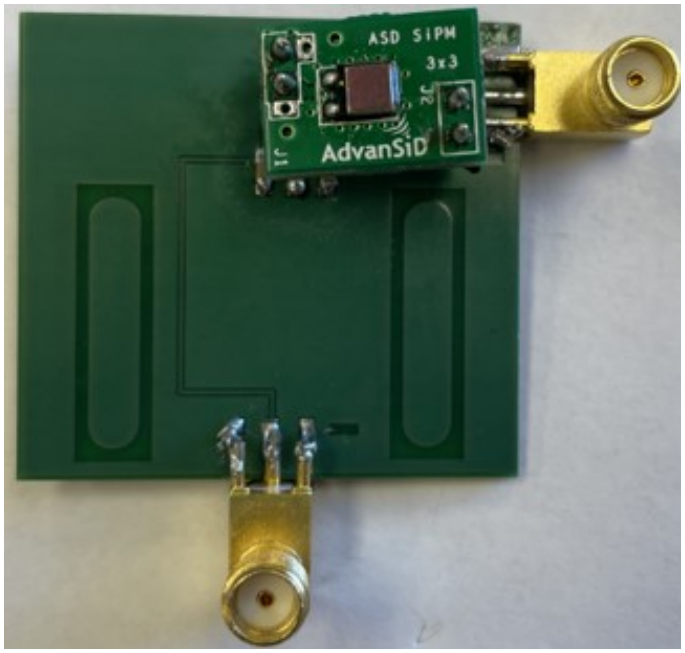

Fig. 7: ASD SiPM mounted on evaluation board.

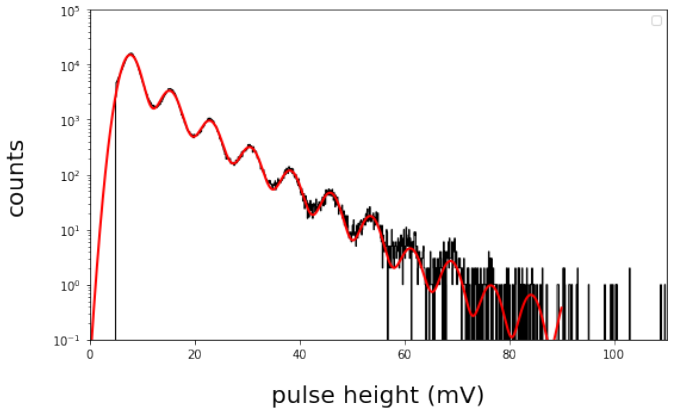

Fig. 8: Dark count spectrum of the MicroFJ30035 SiPM. The red trace is the fit using the modified Erlang distribution.

amount of noise in the ASD could be caused by the denoising step needed for the ASD pulses seen in Fig. 3. The gain of the MicroFJ is 3.5 times higher than the ASD. This can be seen in Fig. 8 by the increased distance between p.e. peaks compared with the distance in Fig. 9.

We also measured the overall dark count rate of the SiPMs and compared them to the values given by the manufacturer. The dark count rate was calculated by noting all signal peaks at or over 1 p.e. amplitude. This value is P in Equation 2. In our case, the duty cycle, d_c is 0.6 and the area (A_s) of both SiPMs is 9mm^2. The calculated values and their comparison are seen in Table III. The data sheet values reported in Table III are found in Ref. [5] and Ref. [6]. We found that the DCR of the MicroFJ was 16% higher than the ASD, which is in good agreement with the data sheet values.

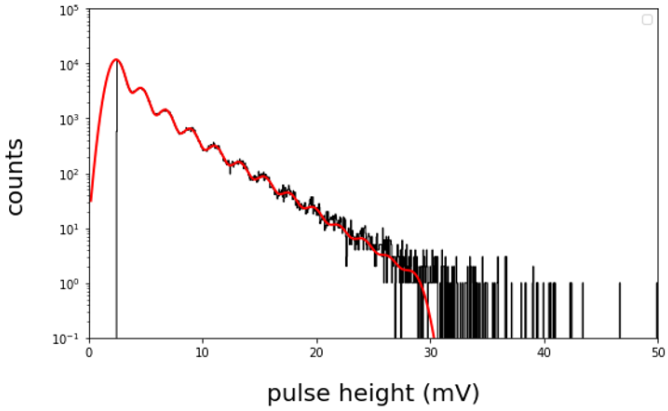

Fig. 9: Dark count spectrum of the ASD-NUV3S-P SiPM. The red trace is the fit using the modified Erlang distribution.

TABLE III: Measured DCR values compared with expected DCR values.

	MicroFJ DCR	ASD DCR
calculated	128kHz/mm^2	110kHz/mm^2
Data sheet value	125kHz/mm^2	100kHz/mm^2

IV. Conclusions

SiPMs are technology that could replace PMTs as photon detectors in some radiation detection scenarios. However, their performance is variable and relies on parameters that must be characterized before they can be used in harsh environments. Parameters such as the SiPMs' DCR, gain, noise, and crosstalk probability affect their response. In this work, we characterized these parameters in two commercial SiPMs (MicroFJ-30035 SiPM by ONSemi and the ASD-NUV3S-P). The DCR of the MicroFJ was measured to be 16% higher than the ASD. Also, the crosstalk probability of the ASD was measured 19.6%, compared to 10.0% for the MicroFJ. Finally, the noise was measured to be significantly higher in MicroFJ. These results agree well with reported values from the manufacturers. The physical parameters of the SiPMs are similar. The MicroFJ has 5,676 microcells with a fill factor of 75%. The ASD has 5,520 microcells with a fill factor of 60%. Importantly for this research, the ASD has a guard ring around its microcells that reduces the dark current, which could lead to an overall reduction in DCR that is seen in this work. In the future, we will add a comparison of a Broadcom AFBR-S4N33C013 SiPM. Additionally, we will characterize the SiPMs' response when coupled with organic scintillators.

References

[1] F. Acerbi and S. Gundacker, "Understanding and simulating sipms," *NIMA*, vol. 926, pp. 16–35, 2019, silicon Photomultipliers: Technology, Characterisation and Applications.

[2] A. Biland, T. Bretz, J. Buß, V. Commichau, L. Djambazov, D. Dorner, S. Einecke, D. Eisenacher, J. Freiwald, O. Grimm, H. von Gunten, C. Haller, C. Hempfling, D. Hildebrand, G. Hughes, U. Horisberger, M. L. Knoetig, T. Krähenbühl, W. Lustermann, E. Lyard, K. Mannheim, K. Meier, S. Mueller, D. Neise, A. K. Overkemping, A. Paravac, F. Pauss, W. Rhode, U. Röser, J. P. Stucki, T. Steinbring, F. Temme, J. Thaele, P. Vogler, R. Walter, and Q. Weitzel, "Calibration and performance of the photon sensor response of fact — the first g-apd cherenkov telescope," *Journal of Instrumentation*, vol. 9, no. 10, p. P10012, oct 2014. [Online]. Available: https://dx.doi.org/10.1088/1748-0221/9/10/P10012

[3] I. Castro, A. Soares, and J. Veloso, “Impact of dark counts in low-light level silicon photomultiplier multi-readout applications,” in *2009 IEEE Nuclear Science Symposium Conference Record (NSS/MIC)*, 2009, pp. 1592–1596.

[4] A. Ghassemi, K. Sato, and K. Kobayashi, “MPPC,” *Hamamatsu technical note*, https://www.hamamatsu.com/content/dam/hamamatsu-photonics/sites/documents/99_SALES_LIBRARY/ssd/mppc_kapd9005e.pdf.

[5] “Silicon photomultipliers (sipm), high pde and timing resolution sensors in a tsv package j-series sipm sensors,” vol. MICROJSERIES/D.

[6] “Nuv sipms chip scale package (csp),” May 2015. [Online]. Available: https://advansid.com/attachment/get/up_28_1432731773.pdf